International Journal of Engineering Research and Technology. ISSN 0974-3154, Volume 12, Number 12 (2019), pp. 2938-2946

Miniaturized Dual Band Antennas with Frequency Tunability for Implanted Biomedical Devices

Adel Damaj[1], Hilal M. El Misilmani[2], and Sobhi Abou Chahine[3]

[1] *Ph.D., Student, Electrical and Computer Engineering Department, Beirut Arab University, Beirut, Lebanon.*
[2] *Assistant Professor, Electrical and Computer Engineering Department, Beirut Arab University, Beirut, Lebanon.*
[3] *Professor, Electrical, and Computer Engineering Department, Beirut Arab University, Beirut, Lebanon.*

Abstract

Antennas miniaturization is a key challenge in the design of implantable antennas for biomedical applications. Attaining a small antenna size, while effectively communicating at low frequencies, can be a major design hurdle. In this paper, a set of miniaturized and tuneable patch antennas is developed. The presented antennas can be tuned to operate at single or multiple frequencies by changing the electrical length. The proposed antennas are of a fixed dimension of $10\times16\times1.59$ mm^3; they can be tuned to operate between 363 MHz and 2.74 GHz. The achieved bands comprise the Medical Implant Communication Service (MICS), Wireless Medical Telemetry Service (WMTS), and the Industrial Scientific and Medical (ISM) radio bands. To validate the attained results, an antenna operating at 1.8 and 2.4 GHz is fabricated and tested in vitro. The obtained results are in accordance with the design objectives.

Keywords: Implantable antennas, Implanted biomedical devices, Miniaturized antennas, Multi-band antennas

I. INTRODUCTION

Antennas for biomedical applications play a great role in the overall implanted biomedical devices. Many studies are done to reach the ultimate implantable antenna design at a desired operating frequency, taking into consideration many factors that play a unique role in the overall design. Implanted medical devices are devices implanted inside the human body, capable of communicating with an external accessory using wireless technology. In the first stages, dual-band electromagnetism used in medical applications, which later diverted into radio frequency (RF) [1], which allows higher data rates and more extended range. Several frequencies bands are recommended to be used in medical implant communications, listed in Table 1.

Nowadays, implanted biomedical devices widely used in many fields, such as continuous real-time pressure measurements, intracranial pressure monitoring, sugar level check, pacemaker connection, radiometer/heating, dental antenna for remote health care applications, insulin push out, endoscopy, and blood pressure measurements. They are essential in human treatment, prevention, and diagnosis.

Table 1. Frequency bands of medical implant communication

Frequency Band	Frequency range
(MICS): Medical Implant Communications Services	401–406 MHz
(WMTS): Wireless Medical Telemetry Service	608-614 MHz, 1395-1400 MHz, and 1427-1432 MHz
(ISM): industrial, scientific and medical radio bands	clustered around 2.4 GHz
(UWB): Ultra Wide Band	3.1-10.6 GHz.

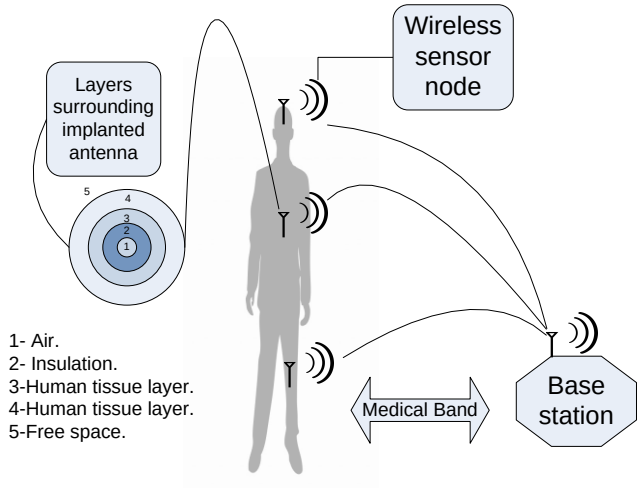

Fig. 1. Wireless implantable system.

Nowadays, implanted biomedical devices widely used in many fields, such as continuous real-time pressure measurements, intracranial pressure monitoring, sugar level check, pacemaker connection, radiometer/heating, dental antenna for remote health care applications, insulin push out, endoscopy, and blood pressure measurements. They are essential in human treatment, prevention, and diagnosis,

A typical implantable biomedical system we have shown in Fig. 1. It generally comprises implantable antennas with its feeding mechanism, surrounded with several layers such as air, insulating layer necessary for safety issues, human tissue layer, and free air, in addition to a base station located outside the

body to receive the transmitted signal from inside the body. Antennas are considered one of the significant parts of implantable devices. Patch antennas are witnessing great attention in such applications due to their high resilience in design, adaptability, and shape solved issues related to patient safety, miniaturization capability, enhanced aspect of communication with external control systems, in addition to biocompatibility.

For the antenna to be implantable and able to be used in biomedical applications, it must be compact [2], capable of being inserted in an implantable device, and designed to operate at a specific frequency band. Many aspects must be studied to ensure full implanted communication system [3] [4], such as the receiver and its sensitivity, the scattering due to surrounded objects and its effect on the path propagation of the radiated EM waves, in addition to the power needed for the implanted antenna, which usually requires the largest size in implantable device. Other challenges facing the design of such antennas are related to the attenuation due to the hostile environment of human bodies [5], such as tissues, bones, and skin, which leads to a reduction in efficiency and bandwidth. Miniaturization of the antenna might also affect its radiation characteristics, and as such, a compromise usually made between radiation characteristics and the size of the antenna.

An implantable CPW fed monopole antenna with a rectangular patch element of dimensions of $18\times24\times0.65$ mm^3 has been presented in [6]. The antenna can operate at a frequency of 2.45 GHz, with a bandwidth of 320 MHz, covering the ISM band. An implantable slot dipole antenna operating in the 2.4 to 2.48 GHz band has also been presented in [7]. The antenna has the dimensions of 18.5×25.9 mm^2. In [8], a miniaturized antenna of the total size of $7\times7\times0.2$ mm^3 has proposed for biomedical applications. The presented antenna operates in the industrial, medical, and scientific 2.40 – 2.4835 GHz band. In [9], two implantable antennas have proposed: a three folded meander antenna with dual-band at 394 MHz and 2.4 GHz with total dimensions of $3.04\times10\times17.25$ mm^3, printed on Rogers 3003 substrate; and a comb antenna of overall size of $1.4\times12\times1.2$ mm^3, printed on Rogers 3210 substrate with bandwidths of 120 MHz and 320 MHz at 418 MHz and 2.43 GHz resonance frequencies. To reduce the losses encountered while using matching circuits, a reconfigurable dual-band antenna using MEMS switches with differential feeding proposed in [10].

In this paper, a miniaturized meandered line patch antenna with an ability to operate at a single or dual frequency bands, with frequency tenability, is presented. The proposed antenna has total dimensions of $10\times16\times1.59$ mm^3, which makes it of dual-band challenging size compared to other implantable antennas operating in the same frequency ranges. Based on changing the length of the meandered antenna, different frequency ranges can be obtained. Monopoles are also used to further decrease the resonant frequency to around 360 MHz. A parametric study is presented to show the design procedure adopted to reach the dual antenna operation at a small antenna size. A mathematical model is further derived that relates the electrical length of the antenna and the operating frequency. Comparing the proposed antenna to similar antennas offered for implanted biomedical applications, the importance of the proposed design procedure is seen in the achieved miniaturized size at low operating frequencies, and with dual-band operation. As a proof of concept, an antenna operating at 1.8 and 2.4 GHz has been fabricated and tested in vitro using pork meat that can mimic the electric properties of the human tissues.

The rest of the paper is organized as follows; Section 2 presents the general design perspective of implantable antennas. Sections 3 describes the proposed antenna design strategy and results. Section 4 presents the fabrication and testing of one of the designed antennas.

II. Design Perspective of Implantable Antennas

Typically, implantable antennas are designed to operate at lower frequency ranges to decrease the penetration loss due to the transmission of the wave from inside the body to the outside receiver [11]. Working at lower frequencies, however, results in large antenna sizes, not suitable for implantable medical devices. As such, reducing the size of the antenna is a significant challenge in the design of antenna ideal for implantable applications [12]. To reach small dimensions, several miniaturization techniques can be used [13], such as:

Choosing suitable dielectric material [14]: high dielectric substrate/superstrate is the simplest way to achieve antenna size reduction. A proper dielectric material can decrease the useful wavelength and hence make smaller resonance frequencies without the need to increase the total size of the antenna [15]. Table 2. lists the different dielectric materials used in the referenced papers with their corresponding dielectric constants. In this paper, FR4 with a thickness of 1.56 mm used due to the simplicity of finding it locally.

Antenna structure: different antenna types and structures can lead to size reduction such as meandered lines, spiral, PIFA, and slot PIFA, dual folded, helical, fractal, and loop antennas [16]. The main aim of these types is to elongate the length of the antenna while keeping the total volume fixed. Table 3. compares some antenna design structures at the same resonance frequency. Table 3 lists different antenna design structures used for implantable medical devices, with their corresponding frequency ranges and dimensions.

Impedance matching: the size of the antenna can also be reduced by optimizing the impedance matching at the desired frequency of operation. Inductance and capacitive loading methods can be used for this aim [17].

In addition to size reduction, one of the critical challenges in designing implantable antennas is to make sure that they are suitable to be implanted inside the human body without affecting their radiation characteristics. For this, the antenna should be tested in simulation software in an environment similar to that of the human tissues [18]. In Fig. 1, a layered model representing the different layers of the body, such as air, insulating layer necessary for safety issues, human tissue layer, and free air, typically used in antennas testing and simulations, is shown. Various simulation software that provides a dynamic

environment for the analysis and simulation of antennas suitable for implanted biomedical applications are found. Table 4 lists the simulation software packages used in the referenced papers.

To test the antenna, two measurement types are usually found: in vitro and in vivo measurements. In vitro measurements, phantoms are used to mimic the electric properties of the human body, and the antenna tested inside of it. Different phantoms have been proposed and used in the literature survey, such as: a liquid similar to the dielectric typical feature of muscle tissue, an equivalent body medium, Polyacrylamide scalp phantom and saline, dental model, a tissue-emulating material consisting of ultra-pure water, sugar, and salt, a heterogeneous sample of a male child from a virtual family, and pork skin phantom [19]. In vivo measurement, animals or the body of human volunteers used for testing the antenna. Table 4 also lists the in vivo measurements setup used to simulate and test the proposed antennas for implanted medical applications.

Table 2. Comparison between different antenna dielectric materials used in reference papers.

Ref.	Materials	Relative dielectric constant ε_r
[20]	alumina ceramic (Al2O3)	9.9
[12]	Rogers 3210	10.2
[21]	ZrO2	21
[6]	ceramic	9.8
[22]	material	4
[16]	Glass wafer	3.7 – 10
[23]	Rogers 4003	3.55
[24]	FR4	4.7
[25]	Roger	10.2
[26]	Teflon, HIK500,	11
[27]	material	2.2

Table 3. Comparison between different antenna structures and frequency bands used in reference papers

Ref.	Dimension (mm)	Design Type	Frequency Band
[26]	14×14×15.	Spiral	MICS
[28]	19 ×30 ×1.6	Slot PIFA	ISM, MICS,WMTS
[29]	8.5×25.9×3.2	Folded slot dipole	ISM
[23]	15×15	PIFA	ISM
[27]	25×34×2.53	Dual folded	ISM, WMTS
[21]	11.5×8×8	Fractal Arc. spirals	MICS
[30]	15×4.5	Helical	868 MHz
[6]	18 × 24 × 0.65	Inverted L- shaped slot, inverted U- shaped slot	ISM
[22]	65×40	PIFA	MICS
[16]	5×3×1	MEMS	1 MHz
[7]	18.5×25.9	Slot Dipole	ISM
[31]	5.3 ×3.25	Meandered PIFA	ISM
[32]	0.16	Loop antenna	4 GHz
[12]	15×15×1.92	L- Shaped fed spiral	ISM, MICS
[25]	30×30×1.6	Dual - spiral	ISM
[20]	14×14	Magnetic-type loop	MICS
[33]	250 ×250	Patch	MICS

Table 4. Simulation software and measurements used in reference papers.

Ref.	Simulation tool	In Vitro Measurements
[26]	HFSS	Equivalent body
[28]	FEKO	Pork skin phantom
[29]	2.5 field simulator	Liquid mimicking tissue
[23]	HFSS	Polyacrylamide, scalp phantom, saline,
[27]	IE3D	Liquid mimicking tissue
[21]	HFSS	dental model
[30]	NA	Testing rig
[6]	IE3D	Water, sugar, and salt
[22]	IE3D	NO
[7]	NA	Child, Virtual Family
[32]	HFSS	Anechoic chamber
[12]	HFSS	The three-layered lossy human tissue model
[25]	CST	human body phantom
[33]	IE3D	NO

III. Antenna Design Strategy and Results

The initially proposed antenna is shown in Fig. 2. with overall dimensions of 10×16 ×1.59 mm^3. The simulations in this section are done using CST software, considering tissue layers, skin, fat, and muscle in the body model. Meander lines are used in the design to have the capability of extending the electrical length of the radiator and hence, achieving resonance at lower frequencies, in addition to frequency tunability. FR4, with permittivity of 4.7, is chosen for the substrate. The different antenna parameters are listed in Table 5. A detailed parametric study is presented in this section to show the steps taken to reach the dual-band antenna suitable for biomedical applications with a miniaturized size. The parametric study includes varying the length of the meander line, adding monopoles, varying the width of the meander line, and varying the spacing between the meander lines. Mathematical functions relating to the length of the radiator and the operating frequency of the antenna are also derived. The parametric study is done to reach dual-band operation at low-frequency bands, suitable for biomedical applications, with miniaturized total dimensions.

III.I Varying the Length of the Meander Line

The first parametric study of the proposed design done on changing the length of the radiator. Several simulations have been performed while varying the number of meander line arms from 6 to 32, in a step of 1 additional arm per simulation Fig. 3. shows the obtained reflection coefficient simulation results for most of the cases studied in Fig. 4. shows the value of the resonance frequency as a function of the total length of the meander line antenna. As can be seen, as the length increases, the resonance frequency decreases. This relation can be modelled using the following equation:

$$f = 2.76 - 0.006 * L$$

Where f is the resonance frequency of the antenna, and L is the total length of the meander line antenna.

It is observed that at (18) meandered line, which is equivalent to 157.6 mm, three resonant frequencies can be achieved, as shown in Fig. 5. Two of these frequencies, 1.4 GHz (WMTS) and 2.4 GHz (ISM), are suitable for biomedical applications.

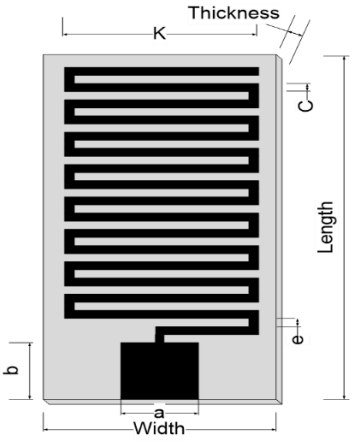

Fig. 2. Patch antenna

Table 5. Antenna dimensions.

Parameter	Dimension (mm)
Width	10
Length	16
Thickness	1.56
a	2.50
b	2.60
c	0.2
e	0.2
k	9.20
z	1
d	1.4
g	15

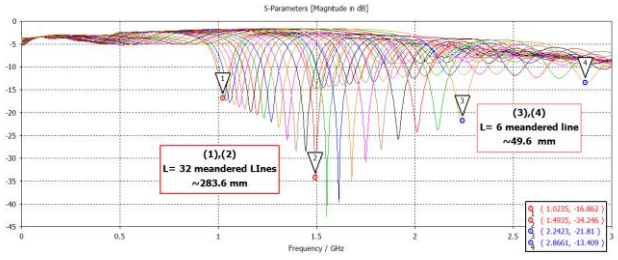

Fig. 3. Simulated reflection coefficient results for different meander line length varying from L_6 ~49.6 mm and L_{32} ~ 283.6 mm.

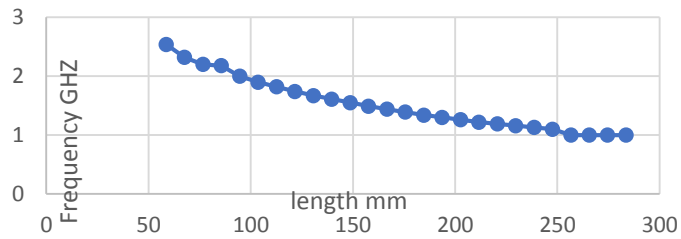

Fig. 4. The relation between the first resonance frequency and different meandered line length.

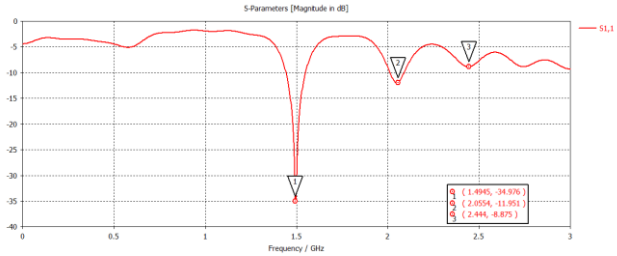

Fig. 5. S11 for18 meandered line length.

III.II Adding Monopoles

The second parametric study is adding monopoles to the proposed design, intending to further decrease the lowest resonance frequency. Three cases are studied: Case 1 having the added monopole to the left of the meander line, as shown in Fig. 6(a), Case 2 having the added monopole to the right of the meander line, as shown in Fig. 6(b), and Case 3 having both monopoles, at the left and right of the meander line, as shown in Fig. 6(c). Each monopole is extended to the edge of the substrate. In a later study in this section, the length of the monopoles is also varied for optimization purposes. Simulating the three different cases, Fig. 7 shows a comparison of the simulated reflection coefficient results for the three different cases studied. Inspecting the graphs, it can be clearly seen that adding both monopoles, to the right and left of the meander lines, achieves a very low resonance frequency compared to the size of the antenna, suitable for operation in the MICS band.

In a further study, Case 3 has been also varied by changing the length of the two monopoles through three different values: quarter-length, half-length, and full-length of 9.2 mm when the monopoles are extended to the edge, as shown in Fig. 8. Fig. 9 shows the simulated reflection coefficient results of all the three different values of monopoles length, compared to the case of having no added length. It can be seen that the full-length monopoles achieve the lowest resonance frequency.

The same parametric study on the length of the meandered lines antennas is done here, with the two added monopoles extended to the edge of the substrate. Fig. 10 shows the simulated reflection coefficient results while varying the length of the meander line. It can be seen that the lowest frequency ranges from 0.3 GHz to 1.44 GHz. Fig. 11 shows the value of the lowest resonance frequency as a function of the total length of the meander line, taking into account the presence of two fully extended monopoles. This relation can be described as follows:

$$f = 1.2 - 0.003 * L$$

where f is the resonance frequency, and L is the full length of the meander line.

It is observed that at a meander line length of 193.6 mm, two resonant frequencies can be achieved, as shown in Fig. 12. Two of these frequencies are suitable for biomedical applications, at 405 MHz (MICS band) and 1.3 GHz (WMTS band).

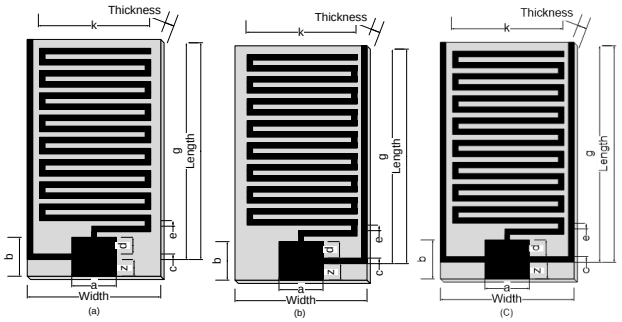

Fig. 6. (a) left monopole antenna, (b) right monopole antenna,(c) left and right monopoles.

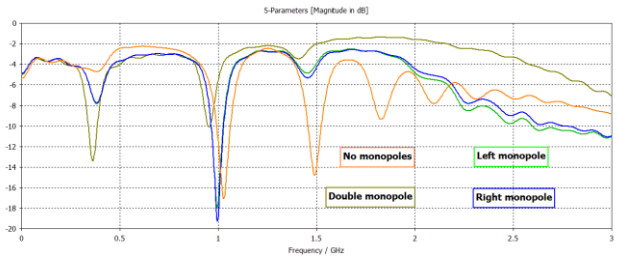

Fig. 7. Comparison of the simulated reflection coefficient results for the different studied cases.

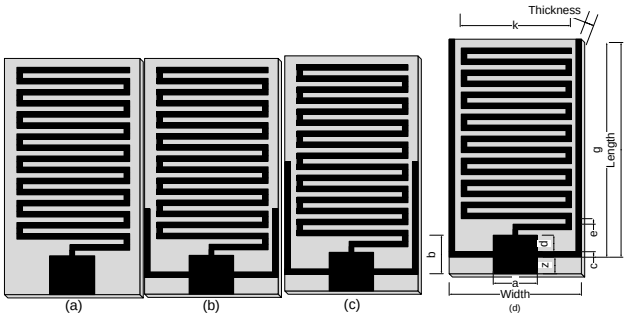

Fig. 8. (a) no monopole, (b) quarter monopole, (c) half monopole, (d) full monopole.

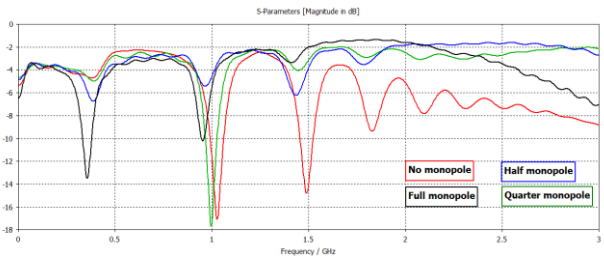

Fig. 9. Different monopole length antennas results.

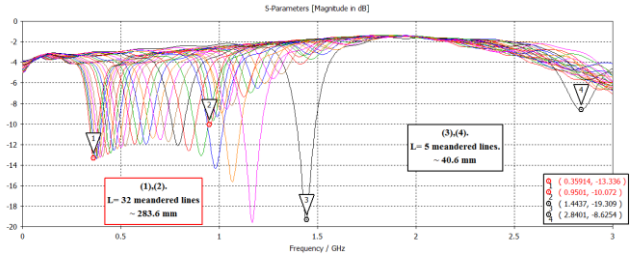

Fig. 10. The simulated reflection coefficient results of Case 3 with fully extended monopole while varying the length of the meander line.

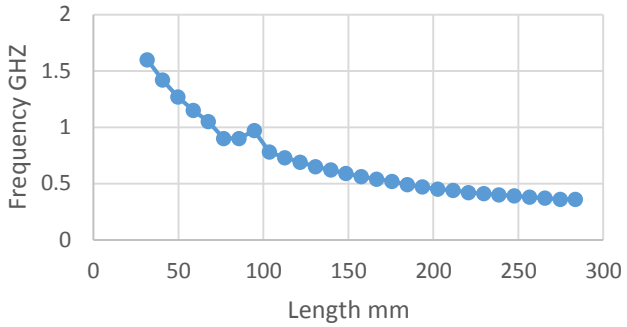

Fig. 11. The relation between the first frequency and different meandered line length for the antenna with two monopoles.

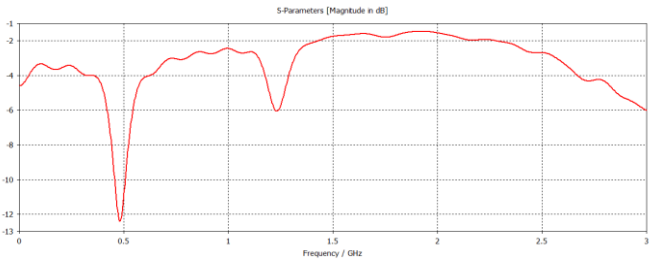

Fig. 12. Simulated reflection coefficient for a total meandered line length of 193.6 mm with two monopoles.

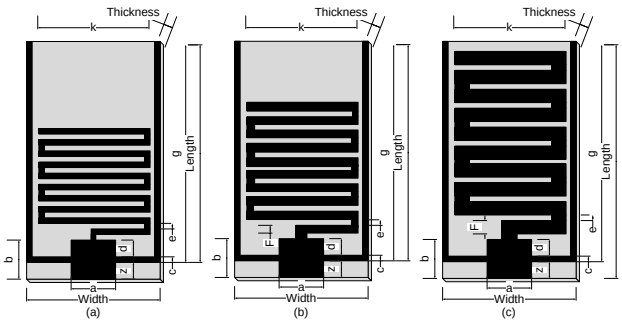

Fig. 13. Different line thickness antennas, (a)0.2mm, (b) 0.4mm, (c) 0.6 mm.

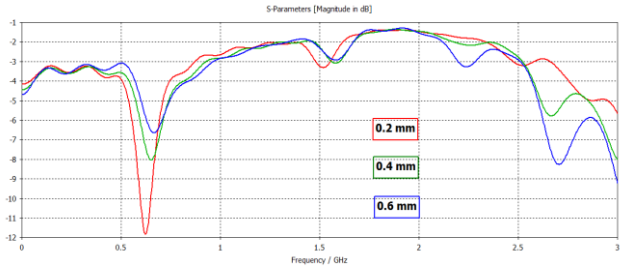

Fig. 14. The simulated reflection coefficient results for three different meander line thickness values, 0.2. 0.4, and 0.6 mm.

III.III Varying the Width of the Meander Line

The third parametric study is done by varying the width of the meander line Fig. 13. Three different thickness values are studied: 0.2, 0.4, and 0.6 mm, as shown in Fig. 14. shows the simulated reflection coefficient results of the three different thickness cases. It is seen that using a thinner width of 0.2 mm, better resonance is achieved at the desired lower frequency.

III.IV Varying Line Spacing

The fourth parametric study is done by varying the separation between the meandered line arms for three different values: 0.2, 0.4, and 0.6 mm, as shown in Fig. 15. Fig. 16 compares the simulated reflection coefficient for the three cases. It can be observed that as the separation between the arms increases, the resulting resonance frequency decreases. More specifically, at 0.6 mm spacing between the meandered lines, a dual-band at 0.4 GHz (MICS band), and 1.3 GHz (WMTS band) achieved. To further optimize the reflection coefficient results at this thickness, especially at the 1.3 GHz resonance frequency, the start of the added monopoles has been shifted through the length of the feed line, with optimized results seen when the monopoles are connected at the end of the line feed, as shown in Fig. 17. The resulting optimized reflection coefficient for this case is shown in Fig. 18.

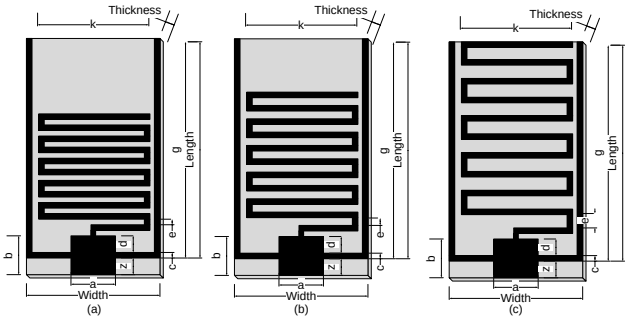

Fig. 15. Different thickness spacing between meandered lines for (0.2, 0.4 and 0.6 mm) antennas.

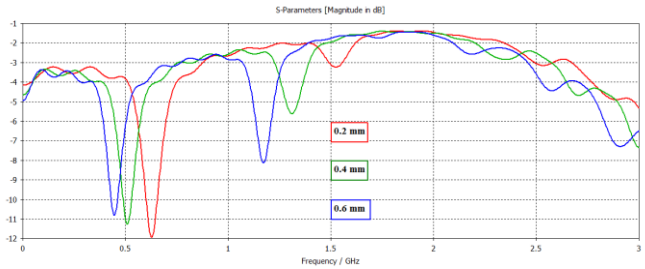

Fig. 16. Different thickness spacing between meandered lines for (0.2,0.4 and 0.6mm) antennas results

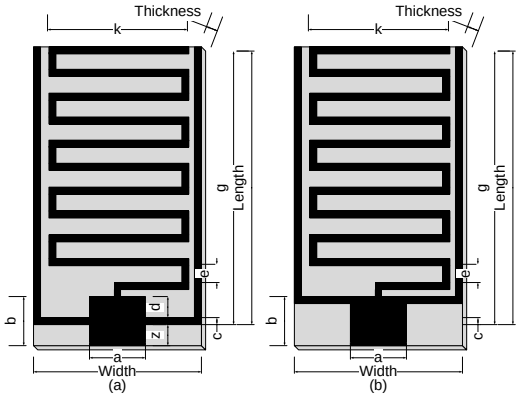

Fig. 17. Shift the point where the monopoles connected with the feed.

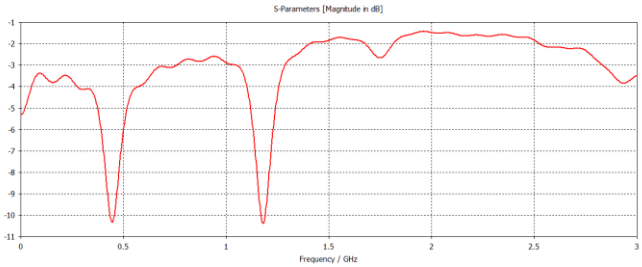

Fig. 18. S11 for 0.6 mm spacing where the monopoles moved.

Finally, checking the reported design in Table 3, the significance of the proposed work is clearly seen in terms of the major size reduction at the very low operating frequency, with dual-band of operation. None of the studied antennas collect the advantages of planar structure, design simplicity, and compact size in one package as the proposed antenna in this work.

IV. Fabrication and Testing

To further validate the proposed design strategy, one of the designed antennas in previous sections is fabricated and tested in vitro. The proposed antenna with 13 meandered line arms, shown in Fig. 19(d), with a total meander line length of 112.6 mm, has been fabricated. The chosen antenna achieves dual-

resonance, at 1.8 and 2.4 GHz bands, with the 2.4 GHz frequency widely used frequency for biomedical applications.

To test the antenna in an environment with electric properties close to those of human tissues, the antenna has been inserted into pork meat, as shown in Fig. 19(b). Fig. 20. Shows a comparison of the simulated reflection coefficient results and the measured one in vitro. As can be seen, the simulated and measured results are in agreement, with some minor differences in the value of the reflection coefficient as a result of soldering, fabrication, and tissue effect. Fig. 21, Fig. 22. Show the simulated gain pattern plots at 1.8 GHz and 2.4 GHz, respectively, with a total gain of 2.54 and 3.39 dBi.

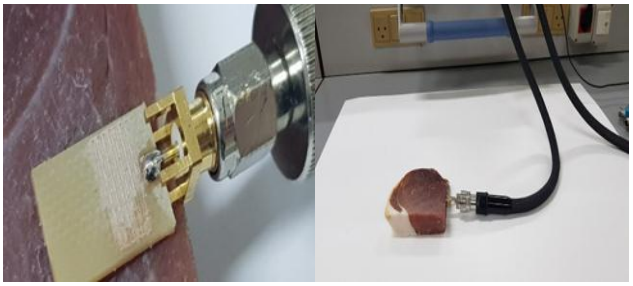

20 a 20 b

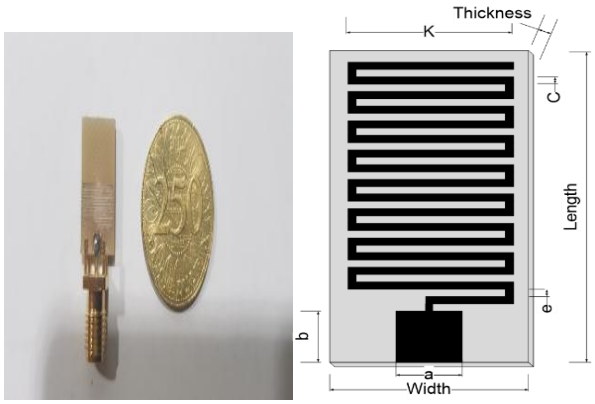

20 c 20 d

Fig. 19. Antenna fabrication and measurements, (a) fabricated antenna. (b) measurements. (c) size. (d) antenna design.

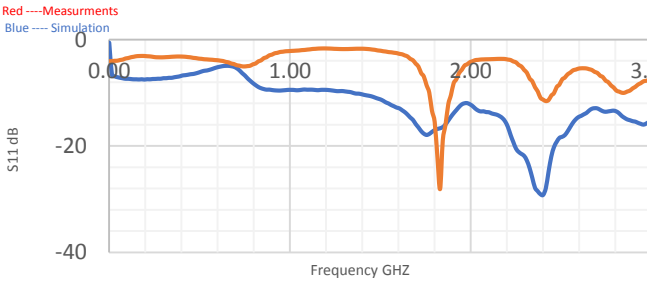

Fig. 20. Comparison of the simulated and measured reflection coefficients results.

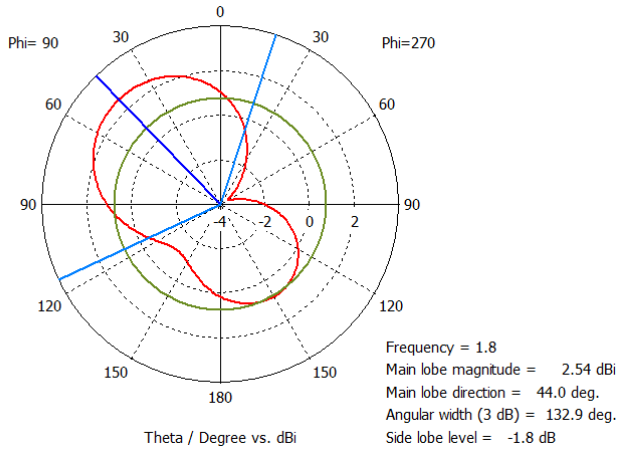

Fig. 21. Radiation pattern at 1.8 GHZ.

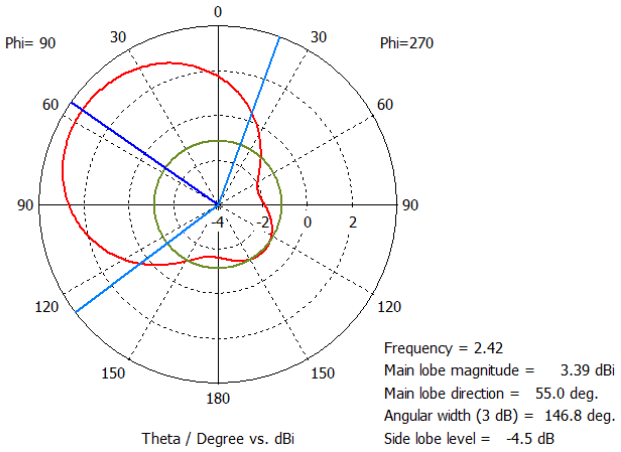

Fig. 22. Radiation pattern at 2.4 GHZ.

V. CONCLUSION

In this paper, the design of single and dual-band antennas of a miniaturized size suitable for biomedical applications is investigated. The article starts with an overview of the design challenges of implanted antennas, investigating the different techniques that can be used to reduce the size for proper insertion inside the body. A set of miniaturized meandered line antennas is developed and simulated. A parametric study has been illustrated that studies the effect of several antenna parameters on the radiation characteristics of the overall antenna. Several studies have been done with an aim to achieve multi-band resonance at a very small antenna size, such as the total length of the meandered lines, line width, spacing, and monopoles addition. The addition of monopoles further decreased the lower resonance frequency to around 360 MHz. Two mathematical models have been developed to capture the relationship between the antenna electrical length and the resonance frequency in two different antenna designs. The presented design procedure, along with the proposed mathematical models, can be used to design any antenna with a

miniaturized size operating at any desired frequency between 363 MHz and 2.74 GHz. A proposed antenna operating at 1.8 and 2.4 GHz has been also fabricated and tested in vitro using pork meat, where good analogy has been seen between the simulated and measured reflection coefficient results.

References

[1] *Recommendation ITU-R RS.1346*, 1998.

[2] G. Kaur, A. Chauhan and G. Kaur, "Implantable antennas for biomedical applications," *International Journal of Engineering Science & Advanced Technology*, vol. 5, no. 3, pp. 198-202, 2015.

[3] K. Gurveer, A. Kaur, G.t Kaur Toor, B. S. Dhaliwal, and S. Sundar Pattnaik, "Antennas for biomedical applications," *Biomedical Engineering Letters 5,no. 3*, pp. 203-212, 2015.

[4] B. Kateryna, and M. V. Jacob, "Implantable devices: issues and challenges," *Electronics*, vol. 2, no. 1, pp. 1-34., 2012.

[5] M. Francesco, B. Fuchs, J. R. Mosig, and A. K. Skrivervik, "The effect of insulating layers on the performance of implanted antennas," *IEEE Transactions on Antennas and propagation*, vol. 59, no. 1, pp. 21-31, 2011.

[6] S. A. Kumar and T. Shanmuganantham, "Design of Implantable CPW Fed Monopole Antenna for ISM Band Applications," *Transaction on electrical materials,* vol. 15, no. 2, pp. 55-59, 2014.

[7] K. Divya, M. Scarpello, G. Vermeeren, W. Joseph, K. Dhaenens, F. Axisa, L. Martens, D. Vande Ginste, H. Rogier, and J. Vanfleteren, "In-body path loss models for implants in heterogeneous human tissues using implantable slot dipole conformal flexible antennas," *EURASIP Journal on Wireless Communications and Networking*, vol. 1, p. 51, 2011.

[8] Bashir, Zubair & Zahid, Muhammad & Abbas, Naeem & Yousaf, Muhammad & Shoaib, Sultan & Asghar, Adeel & Amin,Y, A Miniaturized Wide Band Implantable Antenna for Biomedical Application., Research Gate, 2019.

[9] S, Rashed-Mohassel J., "Design and miniaturization of dual band implantable antennas.," *Elsevier*, p. BBE 288 1–7, 2018.

[10] Shankar Bhattacharjee, Santanu Maity *, Sanjeev Kumar Metya, Chandan Tilak Bhunia, "Performance enhancement of implantable medical antenna using," *Elsevier*, vol. 19, pp. 642-650, 2016.

[11] Q. Xianming, Z. N. Chen, T. S. P. See, C. K. Goh, and T. M. Chiam, "Characterization of RF transmission in human body," in *In Antennas and Propagation Society International Symposium (APSURSI)*, 2010.

[12] M. Palandoken, "Compact Bioimplantable MICS and ISM Band Antenna Design for Wireless Biotelemetry Applications.," *Radioengineering*, vol. 26, no. 4, 2017.

[13] K. Asimina and K. S. Nikita, "A review of implantable patch antennas for biomedical telemetry: Challenges and solutions," *IEEE Antennas and Propagation Magazine*, vol. 54, no. 3, pp. 210-228, 2012.

[14] A. k Skrivervik and F. Merli., "Design Strategies for Implantable Antennas," in *In Antennas and Propagation Conference (LAPC)*, Loughborough, 2011.

[15] A. Damaj , S. Abou Chahine and I. Damaj, "The design and implementation of electrically small reconfigurable patch antennas.," in *In GCC Conference and Exhibition (GCC)*, 2011.

[16] F. J. O. Rodrigues, L. M. Gonçalves and P. M. Mendes, "Electrically small and efficient on-chip MEMS antenna for biomedical devices," in *In Antenna Technology (IWAT)*, 2010.

[17] *IEEE Standard for Safety Levels with Respect to Human Exposure to Radio Frequency Electromagnetic Fields 3 kHz to 300 GHz*, IEEE Std C95.1™, 2005.

[18] Adel Damaj, Hilal M. El Misilmani, and Soubhi Abou Chahine, "Miniaturized Implantable Coplanar Waveguide Antenna for Biomedical Applications," in *HPSC*, Dublin, 2019.

[19] P. Blanos, "Miniaturization of implantable antennas for medical applications," National Technical University of Athens, School of Electrical & Computer Engineering, Athens, 2013.

[20] C. Zhi Ning, G. Chao Liu, and T. SP See., "Transmission of RF signals between MICS loop antennas in free space and implanted in the human head," in *IEEE Transactions on Antennas and Propagation*, 2009.

[21] C.-L. Yang, C.-L. Tsai, and S.-H. Chen, "Implantable high-gain dental antennas for minimally invasive biomedical devices," *IEEE Transactions on Antennas and Propagation*, vol. 61, no. 5, pp. 2380-2387, 2013.

[22] S. Shaheen,S. Dharanya, V. Divya, and A. Umamakeswari, "Design of PIFA antenna for medical applications," *International Journal of Engineering and Technology (IJET)*, vol. 5, pp. 127-132, 2013.

[23] M. Tofighi, "Characterization of biomedical antennas for microwave heating, radiometry, and implant communication applications," in *In Wireless and Microwave Technology Conference (WAMICON)*, 2011.

[24] P. Konstantinos , A. Kiourti, and K. S. Nikita, "Biocompatibility of implantable antennas: Design and performance considerations," in *In Antennas and Propagation (EuCAP)*, 2014.

[25] N. Mahalakshmi and T. Azhagarsamy, "Design and development of dual-spiral antenna for implantable biomedical applications," in *Biomedical Research*, 2017.

[26] J. Abadia, F. Merli, and J.-F. Zurcher, "3D-Spiral Small Antenna Design and Realization for Biomedical Telemetry in the MICS band," *Radioengineerng*, vol. 18, no. 4, pp. 1-5, 2009.

[27] Kumar, S. Ashok, and T. Shanmuganantham, "Implantable CPW fed dual folded dipole antenna for biomedical applications," in *In Computing Communication & Networking Technologies (ICCCNT)*, Coimbatore, India, 2012.

[28] G. Farhad and A. S. Mohan, "Miniaturized slot PIFA antenna for tripleband implantable biomedical applications," in *IEEE MTT-S International*, 2013.

[29] S. Maria Lucia, D. Kurup, H. Rogier, D. Vande Ginste, F. Axisa, J. Vanfleteren, W. Joseph, L. Martens, and G. Vermeeren, "Design of an implantable slot dipole conformal flexible antenna for biomedical applications," *IEEE Transactions on Antennas and Propagation,* vol. 59, no. 10, pp. 3556-3564, 2011.

[30] O. H. Murph., M. R. Bahmanyar, A. Borghi, C. N. McLeod, M. Navaratnarajah, M. H. Yacoub, and C. Toumazou, "Continuous in vivo blood pressure measurements using a fully implantable wireless SAW sensor," *Biomedical microdevices*, vol. 15, no. 5, pp. 737-749, 2013.

[31] D. Oumy, F. Ferrero, A. Diallo, G. Jacquemod, C. Laporte, H. Ezzeddine, and C. Luxey, "Planar antennas on integrated passive device technology for biomedical applications," in *In Antenna Technology (IWAT)*, 2012.

[32] L. Huyen, N. Fong, and H. Cam Luong, "RF energy harvesting circuit with on-chip antenna for biomedical applications," in *In Communications and Electronics (ICCE)*, 2010.

[33] S. Manna, "Rectangular Microstrip Patch Antenna for Medical Applications," *International Journal of Advanced Research in Electrical, Electronics and Instrumentation Engineering*, vol. 5, no. 2, 2016.